
Evolution of Surface Morphology during Epitaxial Growth [and Discussion]

D. D. Vvedensky, N. Haider, T. Shitara, P. Smilauer and J. L. Beeby

Phil. Trans. R. Soc. Lond. A 1993 **344**, 493-505

doi: 10.1098/rsta.1993.0103

Email alerting service

Receive free email alerts when new articles cite this article - sign up in the box at the top right-hand corner of the article or click [here](#)

To subscribe to *Phil. Trans. R. Soc. Lond. A* go to:
<http://rsta.royalsocietypublishing.org/subscriptions>

Evolution of surface morphology during epitaxial growth

BY D. D. VVEDENSKY¹, N. HAIDER¹, T. SHITARA^{1,2}
AND P. ŠMILAUER²

¹*The Blackett Laboratory, and* ²*Interdisciplinary Research Centre for Semiconductor Materials, Imperial College of Science, Technology and Medicine, London SW7 2BZ, U.K.*

We examine the type of information that can be obtained from Monte Carlo simulations of epitaxial growth. A basic model will be first introduced and some of the features that make it suitable for describing both atomic-scale processes and large-scale morphologies will be pointed out. The ability of this model to reproduce experimental data will then be addressed. The first example discussed will be growth on GaAs(001) vicinal surfaces, where the density of surface steps on the simulated surfaces reproduces quantitatively the evolution of the reflection high-energy electron diffraction (RHEED) intensity oscillations for appropriately chosen growth and diffraction conditions. This work will then be used as a basis for examining the predictions of the simulated surface morphologies on patterned substrates, based on comparisons with micro-RHEED measurements. Extensions of the basic model to more complex growth scenarios where the atomic constituents are delivered in the form of heteroatomic molecules will also be discussed.

1. Introduction

The increasing emphasis on the atomic-level description of growth kinetics in recent years has brought about the widespread use of computer modelling, usually involving applications of molecular dynamics and Monte Carlo simulations. These methods provide detailed information about the growth of surfaces by taking explicit account of processes such as deposition, surface migration, and adatom attachment and detachment kinetics at clusters and step edges. Simulations can be used to address the atomic-level origins of particular features of the growth and, in favourable circumstances, to identify the experimental conditions that yield a specified mode of growth.

Somewhat surprisingly, it has proven sufficient for many purposes to focus exclusively on the diffusion and incorporation kinetics of single adatoms. Within this context, not only is there an analytic theory of the transition between step flow and two-dimensional island nucleation and coalescence (Ghez & Iyer 1988; Myers-Beaghton & Vvedensky 1991; Fuenzalida 1991) but, for GaAs (001) under sufficiently As-rich conditions, quantitative agreement with reflection high-energy electron diffraction (RHEED) oscillation data (Shitara *et al.* 1992*a*) can be achieved without any explicit reference to the As source (whether As₂ or As₄) in the theoretical model.

This paper will review recent progress in describing growth morphologies by using Monte Carlo simulations of models that include various atomic-scale processes. Results will be presented to illustrate the kind of information that can be obtained

through systematic comparisons between simulations and measurements. Included in the discussion will be direct comparisons between simulations and RHEED (for vicinal surfaces) and micro-RHEED (for patterned substrates). We will conclude with a few words about generalizing these adatom models to growth scenarios where the decomposition kinetics of heteroatomic precursors affect the growth morphology to the extent that the adatom kinetics must be supplemented with processes that reflect the presence of the precursors.

2. Molecular dynamics and Monte Carlo methods

In the molecular dynamics method (Dodson 1990), real-space trajectories of atoms are calculated by numerical integration of Newton's equations of motion. All of the physics is contained in the forces acting on each particle, which are determined by the interatomic potentials for each atomic type in the system. Despite the evident appeal of applying molecular dynamics to epitaxial growth, there are two impediments to the practical implementation of this method. The first is the choice of potential. Developing potentials even for simple systems is a time-consuming and usually empirical task. Potentials for semiconductors, which contain multi-body interactions, are even more difficult to obtain, and so are available only for a few systems, e.g. silicon (Stillinger & Weber 1985; Bolding & Andersen 1990; Balamane *et al.* 1992).

The second limiting feature of the molecular dynamics methods is the time step used between successive evaluations of the forces acting on the atoms and the corresponding adjustments of the atomic positions. All of the dynamical detail of the system is included in this method, so the time step must be shorter than the vibrational period of the individual atoms (*ca.* 10^{-13}). Thus, phenomena that span seconds, which is typically the time taken to grow a monolayer of material, must be collated from events that each span 10^{-13} s. Consequently, molecular dynamics simulations of epitaxial growth must use unrealistically high growth rates to deposit a significant amount of material during the 'real time' of the simulation.

An alternative to molecular dynamics simulations, where all kinetic processes are obtained as consequences of a particular interaction potential, is an approach where only the rate-determining processes are included. The rates K corresponding to individual processes at the (local) temperature T are usually taken to be of the Arrhenius form,

$$K(T) = K_0 \exp(-E/k_B T), \quad (1)$$

where K_0 represents an attempt rate for the process, E is the barrier for the process, k_B is Boltzmann's constant, and T is the temperature. There is overwhelming evidence (Zangwill 1988; Zhdanov 1991) for the validity of (1) for a variety of surface processes.

The Arrhenius expression (1) requires assigning values to the attempt frequency and to the barrier for a particular process. If it was possible to isolate the effects of an individual process, then these parameters could be determined directly from experimental measurements (Zangwill 1988; Zhdanov 1991). However, by considering only the processes that are expected to be rate-determining, values for K_0 and E must be obtained either from physical arguments, or inferred indirectly by comparing a particular result of the model with experiment. It is important to emphasize that the omission of fast processes which are not rate-determining means that K_0 and E are to be regarded as effective parameters, since the omitted process

could influence the values of these parameters without affecting the qualitative features of the model.

Much of the work using this philosophy for problems in crystal growth has been based on Monte Carlo simulations of lattice models. In this approach, atomic sites are fixed positions on a lattice and the kinetic processes that cause transitions among these sites are described by Arrhenius rates. A conventional Monte Carlo simulation proceeds by calculating the probability distribution of a physical event or series of events based on the expression for the rates. A random number is then generated from a uniform distribution in the interval $[0, 1)$ and compared with the probability of the event occurring. If the random number is greater than or equal to the probability, the event occurs, otherwise not. Such simulations were first applied to crystal growth near equilibrium by Weeks & Gilmer (1979). Review of work directed specifically to the growth morphology of semiconductors have been given by Madhukar & Ghaisas (1988), Das Sarma (1990), Vvedensky *et al.* (1990), and Metiu *et al.* (1992).

The primary advantage of the Monte Carlo over the molecular dynamics method is that comparisons with experiments are easier to make because simulations can be carried out under realistic growth conditions. The molecular dynamics methods can be used to calculate energy barriers for particular kinetic processes, determine relative likelihoods of different events, and even provide detailed information concerning growth mechanisms in the early stages of growth. Although the Monte Carlo method cannot be used to address atomic-level effects that are too specific, it does provide a framework within which to identify the large-scale and long-time consequences of a given potential.

3. The solid-on-solid model of epitaxial growth

We have adopted a model for epitaxial growth (Clarke & Vvedensky 1987) that is close in spirit to the original work of Weeks & Gilmer (1979). The substrate is assumed to have a simple cubic structure with neither vacancies nor overhangs permitted. Thus, every atom has an atom beneath it – the so-called solid-on-solid (sos) criterion. Growth is initiated by the random deposition of atoms onto the substrate, i.e. atoms are added randomly to the individual columns of atoms at each site. The subsequent migration of surface adatoms is taken as a nearest-neighbour hopping process whose rate is

$$k(T) = k_0 \exp(-E_D/k_B T), \quad (2)$$

where k_0 corresponds to an adatom vibrational frequency and E_D is the hopping barrier. The prefactor k_0 is usually taken either as $k_0 = 2k_B T/h$, where h is Planck's constant, or assigned a constant value ($\approx 10^{13} \text{ s}^{-1}$). The simplest form of the hopping barrier is comprised of a term, E_S , from the substrate, and a contribution, E_N , from each nearest neighbour along the substrate. Thus the hopping barrier of an n -fold coordinated atom ($n = 0, \dots, 4$) is $E_D = E_S + nE_N$. This barrier is assumed to depend only on the initial environment of the migrating atom and only surface atoms are assumed to be active. The quantities E_S and E_N are the only free parameters of the model.

In attempting to develop a model with as few free parameters as possible while retaining the essential features of the growth kinetics, some simplifying assumptions have been introduced. Those that require the closest examination are as follows. (i)

The mobility of adatoms is isotropic, in that the nearest-neighbour hopping of each atom is chosen with equal likelihood in all directions regardless of the environment. (ii) The group V kinetics are not included explicitly in the model, since it is assumed that under normal growth conditions the group V species is present in sufficient quantities to insure microscopic stoichiometry (Chen *et al.* 1986). (iii) The effects of the surface reconstruction on mobility can be incorporated as part of the effective migration parameters, as for the case of Si(001) (Clarke *et al.* 1991). None of these assumptions is intrinsic to the model, though any improvements inevitably involve additional parameters, which severely impedes the optimization procedure.

4. Morphological model of RHEED oscillations

Shitara *et al.* (1992*a*) made direct comparisons between the SOS model of MBE and RHEED measurements on vicinal GaAs(001) surfaces with different misorientations for a range of temperatures and fluxes near the temperature T_c where growth becomes dominated by step advancement. The substrate and the growth conditions were chosen to conform as closely as possible to the assumptions (i), (ii) and (iii) of the SOS model described in the preceding section. In particular, (i) the surfaces were misoriented toward the [010] direction to reduce the effect of the anisotropy, (ii) the As/Ga ratio was maintained at approximately 2.5 to avoid variations in the effect of the As as a function of each Ga flux and to maintain the 2×4 reconstruction in a fairly wide temperature range near T_c , thus addressing assumption (iii).

To compare experiments and simulations, it is important to choose the appropriate diffraction conditions. To minimize the contribution from the bulk crystal (mainly incoherent scattering) to the specular beam intensity, the incident polar angle must be chosen to insure that the specular beam spot appears far from the 'Kikuchi-like' features. In the measurements performed by Shitara *et al.* (1992*a*), the incident angle was set at 1.0° along the [100] azimuth. This produced the smallest width of the specular beam and RHEED intensity oscillations during growth on the corresponding singular surface whose maxima correspond to monolayer increments of the deposition of Ga.

The chosen diffraction conditions correspond to 'in-phase', or 'Bragg' conditions, for which reflections from adjacent layers add constructively and the kinematic theory yields a (constant) maximum intensity. The choice of 'out-of-phase' or 'off-Bragg' conditions, where reflection from adjacent layers add destructively, would be more favourable for a kinematic calculation of RHEED. However, because of the contribution from incoherent scattering events and the inability to filter the incoherent component from the total specular intensity, a comparison between theory and experiment cannot be carried out systematically for 'off-Bragg' conditions. Thus, for the diffraction conditions employed for this work, the density of surface steps was used as a model for the variations of the RHEED specular intensity during growth.

In figure 1 is shown a comparison between the measured RHEED specular intensity and simulations of the density of surface steps on a vicinal surface with a misorientation of 2° and for the indicated Ga flux. Comparisons between the measured and simulated values of T_c for the two misorientations and several Ga fluxes produced the following optimized energy barriers: $E_s = 1.58 \text{ eV} \pm 0.02 \text{ eV}$ with $E_N/E_s \approx 0.15$. It must again be stressed that these values are effective migration barriers which depend on all of the effects not included explicitly, so these are the

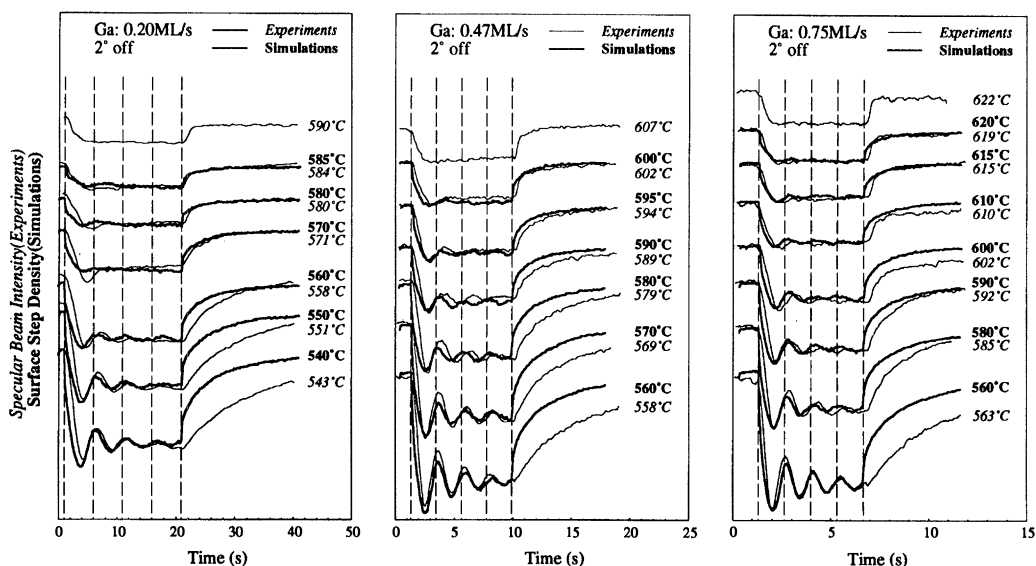


Figure 1. Comparison of measured RHEED specular intensities and step densities from simulated surfaces during growth on vicinal GaAs(001) with a misorientation of 2° for the indicated growth conditions (Shitara *et al.* 1992). The scale of the step densities increases downward and the data for successively higher temperatures are shifted for ease of comparison. The broken lines indicate the points where monolayer increments of the material have been deposited. See text for a discussion of the diffraction conditions.

appropriate barriers only for the specified As/Ga flux ratio. The simulated step density is seen to reproduce several features of the measured RHEED specular intensities, including the decay of the oscillations at lower temperatures, the gradual decrease in the number of oscillations with increasing temperature and the difference between the pre-growth and post-growth amplitudes, and a slight shift of the first maximum with increasing temperature (Shitara *et al.* 1992c).

More striking is the strong degree of quantitative agreement between the two sets of data. The step density in each panel in figure 1 has been scaled by the same factor in order to facilitate comparisons with the RHEED intensities. The agreement in this figure implies that the relative changes of the amplitudes of the two quantities with temperature are the same. This provides strong support for the suggestion by Zhang *et al.* (1990) that the basic processes of diffraction are the same for a surface before growth and during, but that the disorder simply reduces the efficiency of these processes. Additional evidence for the close relationship between the RHEED intensity and surface steps comes from a recent study using scanning tunnelling microscopy (Sudijono *et al.* 1992).

The areas of disagreement between the simulations and the measurements are also important. The régimes where the disagreement is most evident are at the onset of growth and upon recovery at low temperature. Thus, one possible explanation of the disagreement is that the growth is not yet in the steady state, so that As/Ga ratio on the surface is still changing. However, we have no estimates of the effect this has on E_s and E_N , so we cannot say with certainty that this is the origin of the discrepancy.

Another explanation we have investigated is the possibility that step-edge barriers play a role in the growth. Such barriers are known to exist for metals (Ehrlich &

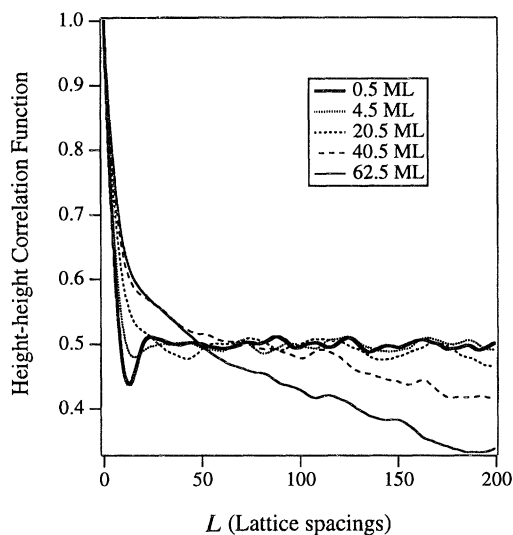


Figure 2. The time evolution of the height–height correlation function, $C(l)$ for the indicated deposition times.

Hudda 1966) and there is some evidence from scanning tunnelling microscopy (Orr 1993) to suggest that they may also exist for GaAs(001). For the growth conditions considered here, we find that by including a small barrier (≈ 0.1 eV), in conjunction with short-range incorporation of freshly deposited atoms (Clarke & Vvedensky 1988; Stoltze & Nørskov 1993), we obtain much better agreement with the RHEED intensity both in the early stages of growth and during recovery over a range of temperatures. However, further work will be necessary to establish unequivocally if the existence of step-edge barriers lies at the root of the discrepancies in the transient régimes.

5. Evolution of surface morphology on singular surfaces

In the early stages of the growth of III–V compounds on nominally flat surfaces, there are oscillations in the specular RHEED spot which exhibit a decaying envelope with time. These oscillations are associated with the formation, growth, and coalescence of two-dimensional islands on the substrate (Neave *et al.* 1985). Thus, on a flat substrate, the initial decrease in the RHEED intensity is due to the formation of islands over large regions of the substrate. The decaying envelope of the oscillations results from the ‘memory’ of the initially flat surface being gradually lost as the growth rates of separate regions become uncorrelated due to the statistical fluctuations of the diffusion and deposition processes. An important implication of this is that the early stages of growth should exhibit a degree of long-range spatial order in the growth front.

To investigate this effect, we have carried out simulations on singular 800×800 lattices with periodic boundary conditions. The morphology of the growing substrate was monitored through ‘snapshots’ of the surface and by calculating a height–height correlation function. The latter quantity is the probability that sites a distance l apart have the same height. To simplify the calculation only distances along the x and y directions were considered. Figure 2 shows this correlation function at various half-layer completion points. There are several features to note. First, 0.5

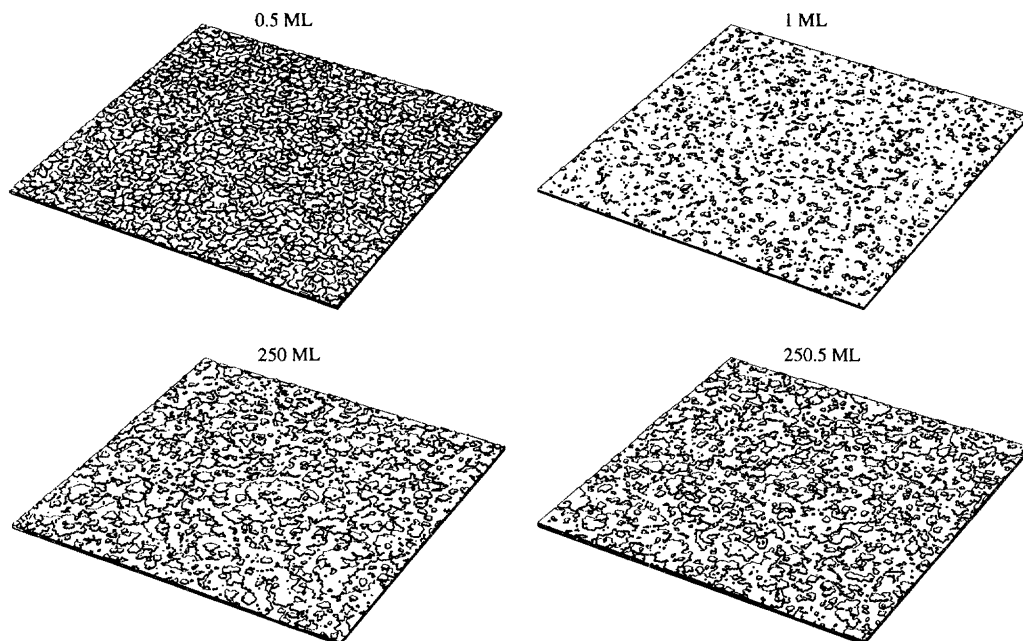


Figure 3. 300×300 sections of 800×800 lattices with periodic boundary conditions after the deposition of the indicated numbers of monolayers. To overcome the artificial restriction of a perfectly flat initial substrate, the simulations were performed on a starting surface prepared by depositing several layers of material and then allowing the system to relax for a period of 20 s. The monolayer completion time is 8 s.

monolayers, there are distinct oscillations in the correlation function. The average island size is found to 12 lattice sites, while the oscillatory part of the correlation function gives an inter-island separation (measured from the centres of the islands) of 12 ± 3 lattice sites. This suggests a morphology where the islands are approximately of equal size with a separation approximately equal to the average island size. Such an ordered morphology in the early stages of growth has also been reported for X-ray scattering studies (Fuoss *et al.* 1992) during MOCVD. As the growth proceeds, this correlated spatial structure begins to decay, and at 62.5 monolayers, the separation of the substrate into weakly correlated regions is becoming increasingly evident.

The decay of spatial correlations during growth can also be seen most by examining the evolution of the surface morphology (figure 3). Near the onset of growth, the surface undergoes large-scale changes in the surface morphology upon the addition of a half-monolayer of material. At a much later stage, the deposition of a half-monolayer has a much smaller effect, since the growth front has roughened. This causes a degradation and eventual loss of the long-range order, as the growth front spreads over an increasing number of layers. The morphologies in figure 3 suggest that the decay of these spatial correlations corresponds to the decay of the RHEED intensity oscillations.

This conclusion is supported by a recent study using scanning tunnelling microscopy (Sudijono *et al.* 1992). In this work, surfaces of GaAs(001) were rapidly quenched during various stages of growth, which enabled the preparation of a surface whose morphology is close to that at the time of the onset of the quench. This study revealed that the decay of the RHEED oscillations occurred without a corresponding

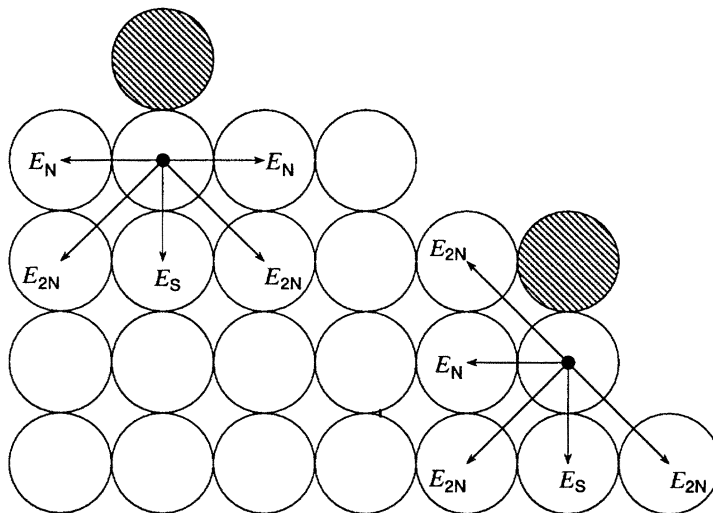


Figure 4. Nearest-neighbour, second nearest-neighbour and surface contributions to the hopping barrier E_D included in the modified sos model to account for the stability of (001) and (111) facets. Single adatoms on the (001) and (111) facets are indicated with shading.

increase in the number of incomplete layers at the growth front. This points to the decay of the RHEED oscillations being due to the evolution of the surface toward a constant step density.

6. Epitaxial growth on non-planar substrates

Most of the theoretical and experimental work to date on epitaxial growth has focussed on singular and vicinal surfaces. However, growth on patterned substrates has attracted interest because of the appearance of features not seen on vicinal or singular surfaces, such as the lateral variations of the growth rate (Smith *et al.* 1985).

In order to consider situations where facets other than (001) are stable, we must modify the basic model discussed in §3. Previous studies (Rottman & Wortis 1984) have shown that interactions among more distant neighbours are required to describe faceting behaviour. Accordingly, to stabilize a (111) facet, the hopping barrier E_D in (2) must be modified to have the following form: $E_D = E_S + nE_N + mE_{2N}$ where n is the number of in-plane nearest-neighbours and m is the number of out-of-plane next-nearest neighbours (figure 4). The neglect of in-plane next-nearest neighbours is only for computational reasons and is not expected to lead to any qualitative differences from the results reported below. In the absence of experiments such as those described in §4 which may be used to estimate these energy barriers, we will use values that are expected to reflect the average morphological behaviour of GaAs based on observations during scanning microprobe RHEED experiments on GaAs (001) near (111) surfaces.

We consider first a simulation with the parameters $E_{2N} = 0.1$ eV, $E_S = 1.0$ eV and $E_N = 0.3$ eV. Since $E_{2N} < E_N$, this choice results in greater mobility of single adatoms on the (001) surface as compared to the diagonal surface (figure 4). Figure 5a shows the effective growth rate. At low temperatures growth occurs in a shape-preserving manner because adatoms cannot easily migrate to the lower energy facet. At higher temperatures, the flat terrace shows a large negative growth rate because free

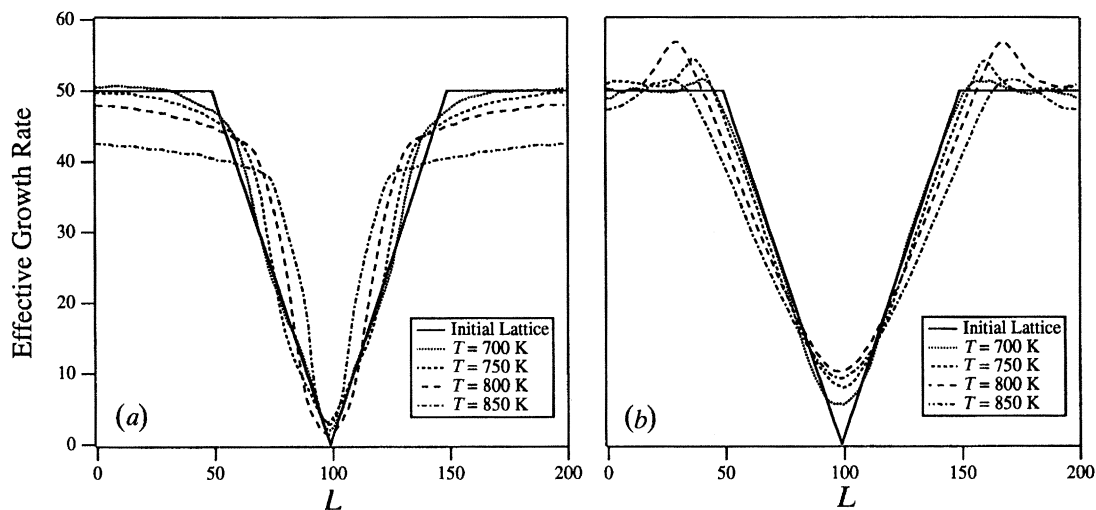


Figure 5. The projected effective growth rate after the deposition of 500 monolayers for the indicated substrate temperatures for (a) greater mobility on the (001) facet and (b) greater mobility on the (111) facet of an sos model. The initial substrate is shown as a reference. The two-dimensional morphology along the groove has been averaged to give a one-dimensional surface profile. The growth rate is simply the average morphology with the number of deposited monolayers subtracted.

adatoms are diffusing across the flat terrace toward the diagonal facet, on which there is a lower mobility. As deposition continues, adatoms diffuse down the diagonal facet, resulting in a positive growth rate deep in the groove. If growth is continued indefinitely the growth front will planarize as the two diagonal facets merge.

Consider now the case where $E_{2N} = 0.38$, $E_S = 0.3$ and $E_N = 0.1$, so $E_{2N} > E_N$. This ensures a greater mobility of single adatoms on the diagonal surface as compared with the (001) surface (figure 4). The value of E_S was changed to maintain a similar temperature scale for both cases. The effective growth is shown in figure 5b. At low temperatures growth again occurs in a shape preserving manner as in the previous case. At higher temperatures, the groove exhibits a negative growth rate since adatoms migrate from the diagonal facet to the flat terrace. This leads to a maximum in the supersaturation at the edge of the flat surface resulting in the formation of a 'lip'. As growth continues the growth front again planarizes as the two diagonal facets diverge, which is the opposite behaviour to that seen for the case discussed above.

These observations are reinforced by real time scanning microprobe RHEED measurements on GaAs(001) near (111)A and (111)B surfaces (figure 6). Experimental data from real time scanning microprobe RHEED measurements (Hata *et al.* 1990) on GaAs(001) near a (111)B show that the period of specular RHEED intensity increased on the (001) surface near the (111)B facet, implying a slower growth rate. The relative growth rate rapidly decreases as a function of the distance from the interface. The experimental results also show that the gradient of the (111)B facet is smaller at higher temperatures, which is also in agreement with the projected morphology in figure 5a.

The corresponding measurements on GaAs(001) near a (111)A surface reveal a higher growth rate, as shown in figure 6b. Near this interface the intervals between the maxima in the reflected intensity are decreasing with time, which implies that the

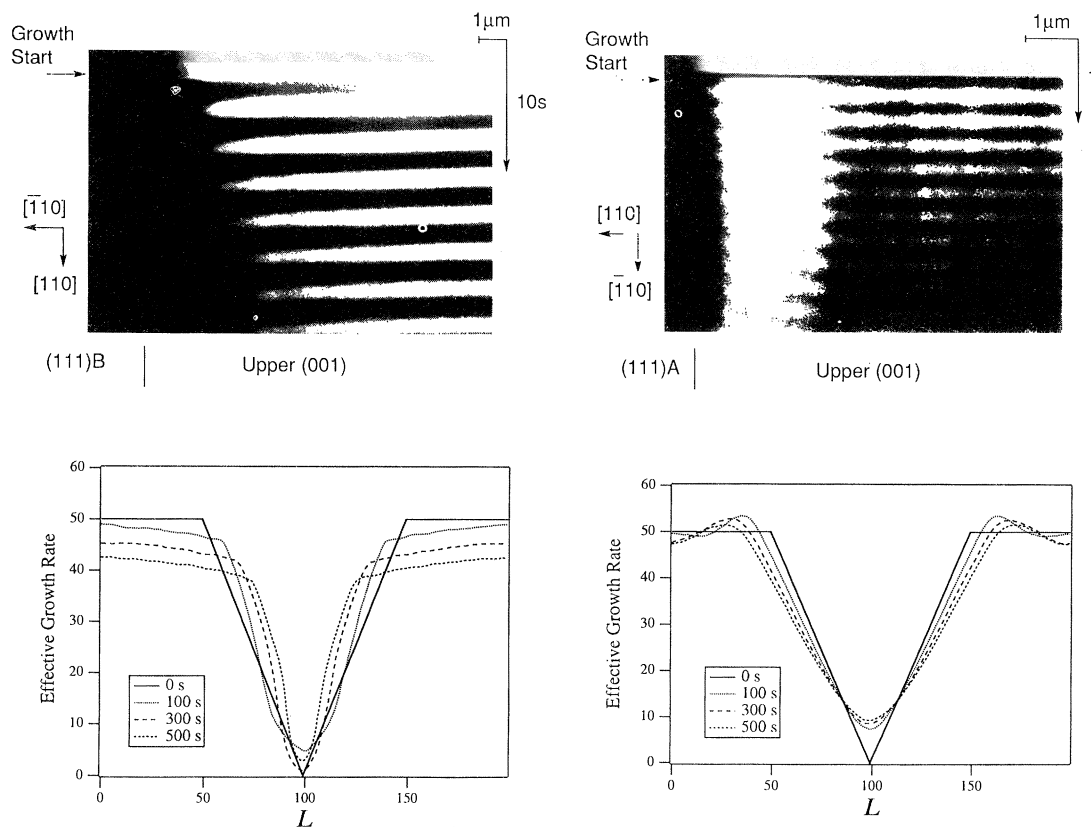


Figure 6. Left panel: comparison between (top) a microprobe RHEED image (Hata *et al.* 1990) of the GaAs surface near the edge of the (111)B surface during growth at a temperature of 450 °C and (bottom) the time evolution of the projected effective growth rate at the indicated times. Right panel: same as the left panel but for a GaAs surface near the (111)A surface during growth at a temperature of 550 °C. In both panels the vertical axis is the time and the stripes correspond to RHEED intensity oscillations.

effective growth rate is increasing, with the gradients of the increases being smaller at higher temperature. All of these observations are in qualitative agreement with the simulated morphologies in figure 5*b*.

7. Precursor-mediated epitaxial growth

The results of the preceding sections show how adatom models can be used to explain a variety of phenomena in epitaxial growth from solid sources. However, there is increasing evidence that these simple adatom models are not adequate to describe the growth kinetics for the general case when the atomic constituents of the growing film are delivered to the substrate in the form of heteroatomic molecules. For example, the very different kinetics observed for surface reactions (Donnelly *et al.* 1991; Yu *et al.* 1991) and growth (Okuno *et al.* 1990; Kaneko *et al.* 1993) when trimethylgallium (TMG) or triethylgallium (TEG) is deposited onto GaAs makes clear that no single universal theoretical model is likely to be appropriate for the epitaxial growth of GaAs in all experimental scenarios.

With the advent of new experiments and diagnostic techniques to monitor growth from precursors (Aspnes *et al.* 1989; Fuoss *et al.* 1992; Kaneko *et al.* 1993), the

possibility now exists to carry out systematic theoretical studies of these growth experiments. In this section we will describe some of our initial efforts at simulating precursor-mediated growth using modified versions of the model described in §3. We will consider two experiments on the growth of GaAs(001) with MOMBE using TEG and TMG sources. For the case of TEG, Okuno *et al.* (1990) measured RHEED intensity oscillations on both singular and vicinal GaAs(001) surfaces and made comparisons with growth from solid-source Ga under nominally the same growth conditions. On a singular surface, the RHEED oscillations measured during MOMBE decayed more slowly than those measured during MBE, but on a vicinal surface, there was no discernible difference.

We have modelled these experiments by adding to our model a precursor (not necessarily TEG) with greater mobility than atomic Ga. The decomposition of this precursor to release a Ga atom is taken to be the rate-determining reaction in the TEG \rightarrow Ga sequence and to be much more facile at a step edge than on a terrace. On a singular surface, the simulated step densities reproduce the qualitative behaviour seen in the measured RHEED intensities, as expected by the presence of a more mobile species. On a vicinal surface, however, the results are more subtle. Although the precursor migrates quickly to a step edge, where decomposition occurs quickly, growth does not necessarily occur by step flow. This is because the Ga atoms released by the decomposition reaction can detach from the step onto the terrace (Shitara *et al.* 1992*c*), where collisions with other Ga atoms lead to island formation, the edges of which act as sites for the decomposition of the precursor. This leads to RHEED intensity oscillations that are similar to those found using the model of §3 under the same growth conditions.

The second MOMBE experiment we will examine is the growth of GaAs(001) from TMG. Previous work on the growth of GaAs(001) from solid sources (Shitara *et al.* 1992*b*) has shown that T_c is greater on a surfaces misoriented toward the [100] direction than those misoriented toward $[\bar{1}10]$ (for the same misorientation angle). Kaneko *et al.* (1993) found that this misorientation-dependence is enhanced when TMG is used. The trends in MBE can be explained by adding an anisotropy in the hopping barrier E_N , i.e. the barrier is greater for neighbours located along the $[\bar{1}10]$ direction than along [110]. The hopping of the precursor is taken to be isotropic. To simulate the experiments with the TMG precursor, we suppose that the decomposition can occur only at an As-terminated step edge, i.e. an edge along the $[\bar{1}10]$ direction, while retaining the anisotropic nearest-neighbour hopping barriers of the MBE model. The results show that the anisotropy of the decomposition rate does indeed enhance the misorientation dependence of T_c found earlier. While this result is suggestive and encouraging, we must point out that other effects such as site-blocking (Kaneko *et al.* 1993) cannot be excluded.

The final example of precursor-mediated growth we will examine concerns the growth of GaAs(001) using MOCVD from TMG. This is a more complicated growth scenario than MBE or MOMBE because the incident beam is hydrodynamic, which means that gas-phase reactions cannot, strictly speaking, be ignored. Recent experiments using glancing-angle X-ray scattering (Fuoss *et al.* 1992) have revealed both similarities and differences when compared with MBE. Most notably, oscillations are seen in the reflected beams, which are indicative of layer-by-layer growth. However, on a substrate with a terrace length of approximately 4900 Å, the oscillations are observed to diminish with increasing temperature and disappear at $T \approx 630$ K, a situation that is usually associated with the transition to growth by

step flow. When compared with MBE on a surface with the same misorientation, this is far too low a temperature for this transition. On the other hand, the submonolayer growth morphology is characterized by a cooperative growth of islands, both in terms of size and distribution (§5).

Our preliminary analysis of these data has focused on identifying differences from predictions based on simulations of MBE. One difference, the value of T_c , was already pointed out. Another difference is provided by examining the temperature-dependence of the average island size, \bar{l} . Various approaches to this problem in MBE have suggested that this behaviour follows the scaling law $\bar{l} = (D/J)^\gamma$, where D is an effective diffusion constant of the Arrhenius form (1) and J is the deposition flux. Estimates for the value of γ range from $\frac{1}{8}$ to $\frac{1}{4}$, depending on the growth conditions (Villain *et al.* 1992). If the same analysis is applied to data of Fuoss *et al.* (1992), a much larger value of γ is obtained, i.e. there is a much larger increase with temperature of the average island size in MOCVD than in MBE. Since these previous analyses are based on growth kinetics that are well-described by considering only deposition and diffusion, this result suggests that growth by MOCVD contains features not included in these models.

N.H. thanks the Science and Engineering Research Council for support. The authors have benefited from discussions with P. H. Fuoss, B. A. Joyce, D. W. Kisker, T. Kaneko, B. G. Orr, M. R. Wilby, and A. Zangwill. Some of the work described here was supported by Imperial College and the Research Development Corporation of Japan through the 'Atomic Arrangement: Design and Control for New Materials' Joint Research Program.

References

- Aspnes, D. E., Bhat, R., Colas, E., Keramidis, V. G., Koza, M. A. & Studna, A. A. 1989 *J. Vac. Sci. Technol. A* **7**, 711.
- Bolding, B. C. & Andersen, H. C. 1990 *Phys. Rev. B* **41**, 10568.
- Balamane, H., Halicioglu, T. & Tiller, W. A. 1992 *Phys. Rev. B* **46**, 2250.
- Chen, P., Kim, J. Y., Madhukar, A. & Cho, N. M. 1986 *J. Vac. Sci. Technol. B* **4**, 890.
- Clarke, S. & Vvedensky, D. D. 1987 *Phys. Rev. Lett.* **58**, 2235.
- Clarke, S. & Vvedensky, D. D. 1988 *Phys. Rev. B* **37**, 6559.
- Clarke, S., Vvedensky, D. D. & Wilby, M. R. 1991 *Surf. Sci.* **255**, 91.
- Das Sarma, S. 1990 *J. Vac. Sci. Technol. A* **8**, 2714.
- Dodson, B. W. 1990 *CRC Crit. Rev. Sol. State Mater. Sci.* **16**, 115.
- Donnelly, V. M., McCaulley, J. A. & Shul, R. J. 1991 In *Chemical perspectives of microelectronic materials II* (ed. L. V. Interrante, K. F. Jensen, L. H. Dubois & M. E. Gross), pp. 15–23. Pittsburgh, Pennsylvania: Materials Research Society.
- Ehrlich, G. & Hudda, F. G. 1966 *J. chem. Phys.* **44**, 1039.
- Fuenzalida, V. 1991 *Phys. Rev. B* **44**, 10835.
- Fuoss, P. H., Kisker, D. W., Lamelas, F. J., Stephenson, G. B., Imperatori, P. & Brennan, S. 1992 *Phys. Rev. Lett.* **69**, 2791.
- Ghez, R. & Iyer, S. S. 1988 *IBM J. Res. Develop.* **32**, 804.
- Hata, M., Isu, T., Watanabe, A. & Katayama, Y. 1990 *J. Vac. Sci. Technol. B* **8**, 692.
- Kaneko, T., Naji, O., Jones, T. S. & Joyce, B. A. 1993 *J. Cryst. Growth*. (In the press.)
- Madhukar, A. & Ghaisas, S. V. 1988 *CRC Crit. Rev. Sol. State Mater. Sci.* **14**, 1.
- Metiu, H., Lu, Y.-T. & Zhang, Z. 1992 *Science, Wash.* **255**, 1088.
- Myers-Beaghton, A. K. & Vvedensky, D. D. 1991 *Phys. Rev. A* **42**, 2457.
- Neave, J. H., Dobson, P. J., Joyce, B. A. & Zhang, J. 1985 *Appl. Phys. Lett.* **47**, 100.
- Okuno, Y., Asahi, H., Kaneko, T., Kang, T. W. & Gonda, S. 1990 *J. Cryst. Growth* **105**, 185.
- Phil. Trans. R. Soc. Lond. A* (1993)

- Rottman, C. & Wortis, M. 1984 *Phys. Rev. B* **29**, 328.
- Shitara, T., Vvedensky, D. D., Wilby, M. R., Zhang, J., Neave, J. H. & Joyce, B. A. 1992a *Phys. Rev. B* **46**, 6815.
- Shitara, T., Vvedensky, D. D., Wilby, M. R., Zhang, J., Neave, J. H. & Joyce, B. A. 1992b *Phys. Rev. B* **46**, 6825.
- Shitara, T., Zhang, J., Neave, J. H. & Joyce, B. A. 1992c *J. appl. Phys.* **71**, 4299.
- Smith, J. S., Derry, P. L., Margalit, S. & Yariv, A. 1985 *Appl. Phys. Lett.* **47**, 712.
- Stillinger, F. H. & Webber, T. A. 1985 *Phys. Rev. B* **31**, 5262.
- Stoltze, P. & Nørskov, J. K. 1993 (In the press.)
- Sudijono, J., Johnson, M. D., Snyder, C. W., Elowitz, M. B. & Orr, B. G. 1992 *Phys. Rev. Lett.* **69**, 2811.
- Villain, J., Pimpinelli, A., Tang, L. & Wolf, D. 1992 *J. Phys. I (France)*, **2**, 2107.
- Vvedensky, D. D., Clarke, S., Hugill, K. J., Myers-Beaghton, A. K. & Wilby, M. R. 1990 In *Kinetics of ordering and growth at surfaces* (ed. M. G. Lagally), pp. 297–311. New York: Plenum.
- Weeks, J. D. & Gilmer, G. H. 1979 *Adv. chem. Phys.* **40**, 157.
- Yu, M. L., Memmert, U., Buchan, N. I. & Kuech, T. F. 1991 In *Chemical perspectives of microelectronic materials II* (ed. L. V. Interrante, K. F. Jensen, L. H. Dubois & M. E. Gross), pp. 37–46. Pittsburgh, Pennsylvania: Materials Research Society.
- Zangwill, A. 1988 *Physics at surfaces*. Cambridge University Press.
- Zhang, J., Neave, J. H., Joyce, B. A., Dobson, P. J. & Fawcett, P. N. 1990 *Surf. Sci.* **231**, 379.
- Zhdanov, V. P. 1991 *Elementary physiochemical processes on solid surfaces*. New York: Plenum.

Discussion

J. L. BEEBY (*University of Leicester, U.K.*). I am concerned at Dr Vvedensky's choice of pre-exponential factor, which is important for a correct description of the surface chemistry involved. He has chosen 10^{13} s^{-1} , which is a free atom value and several order of magnitude too large for atoms or molecules at semiconductor surfaces. It taken no account of bonds or geometrical effects. Clearly this will have a major influence on the results he claims.

D. D. VVEDENSKY. For a variety of *metals*, field-ion microscopy measurements (Tsong 1993) yield a frequency factor in the range of 10^{12} s^{-1} – 10^{13} s^{-1} . The situation for semiconductor surfaces is less clear. Mo *et al.* (1991) used STM to measure the number density of islands formed during deposition and deduced a prefactor of *ca.* 10^{13} s^{-1} . On the other hand, Ganz *et al.* (1992) applied STM to measure Pb atoms diffusing on Ge(111) and found that the pre-factor is several orders smaller than this, primarily because of a cooperative exchange mechanism. Robertson *et al.* (1988) fit growth rates of GaAs with chemical-beam epitaxy using Arrhenius rates for all chemical and desorption process and found all frequency factors were in the range 10^{11} s^{-1} – 10^{14} s^{-1} . Thus, since we are describing the growth kinetics in terms of elementary single-atom processes, a prefactor of *ca.* 10^{13} s^{-1} does not appear unreasonable, particularly in the absence of more definitive experimental and theoretical work.

Additional references

- Ganz, E., Theiss, S. K., Hwang, I.-S. & Golovchenko, J. 1992 *Phys. Rev. Lett.* **68**, 1567.
- Mo, Y. W., Kleiner, J., Webb, M. B. & Lagally, M. G. 1991 *Phys. Rev. Lett.* **66**, 1998.
- Robertson, Jr, A., Chiu, T. H., Tsang, W. T. & Cunningham, J. E. 1988 *J. Appl. Phys.* **64**, 877.
- Tsong, T. T. 1993 *Physics Today* **46**(5), 24.

Phil. Trans. R. Soc. Lond. A (1993)

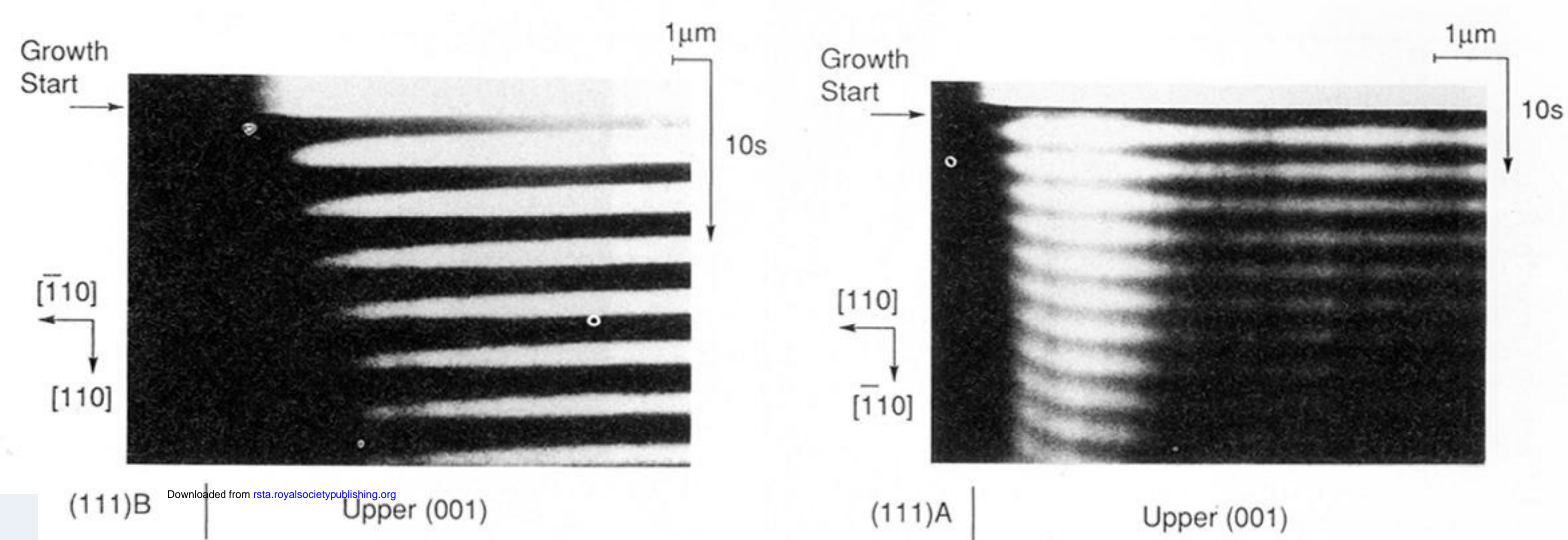


Figure 6. Left panel: comparison between (top) a microprobe RHEED image (Hata *et al.* 1990) of the GaAs surface near the edge of the (111)B surface during growth at a temperature of 450 °C and (bottom) the time evolution of the projected effective growth rate at the indicated times. Right panel: same as the left panel but for a GaAs surface near the (111)A surface during growth at a temperature of 550 °C. In both panels the vertical axis is the time and the stripes correspond to RHEED intensity oscillations.